Journal of Nuclear Materials 377 (2008) 225–231

Contents lists available at ScienceDirect

Journal of Nuclear Materials

journal homepage: www.elsevier.com/locate/jnucmat

Stressed capsules of austenitic and martensitic steels irradiated in SINQ Target-4 in contact with liquid lead–bismuth eutectic

Y. Dai *, D. Gavillet, R. Restani

Paul Scherrer Institut, 5232 Villigen PSI, Switzerland

A B S T R A C T

In the MEGAPIE target, the steels used for the proton beam entrance window and other components in the spallation reaction zone suffer not only from the irradiation damage produced by protons and neutrons but also from the corrosion and embrittlement induced by liquid lead–bismuth eutectic (LBE). Although these effects have been separately studied by a number of authors, the synergistic effects of irradiation, LBE corrosion and embrittlement are little understood. This work presents detailed analyses of two stressed capsules made of the austenitic steel EC316LN and the martensitic steel 9Cr2WVTa, which were irradiated in SINQ Target-4 in contact with LBE at calculated temperatures of 315 and 225 °C, respectively. The Electron Probe Microanalysis (EPMA) on the cross-sections of the capsules showed that the stagnant LBE induced only slight corrosion on both capsules and no cracks existed in the wall of the EC316LN capsule. Some cracks were observed in the electron beam weld (EBW) and its vicinity of the 9Cr2WVTa capsule, which can be attributed to the high stress inside the wall, the hardening of the material induced by either welding (without re-tempering) or irradiation, and the effects of LBE embrittlement.

1. Introduction

In advanced high power spallation targets such as the Mega Watt Pilot Experiment (MEGAPIE) of Swiss Spallation Neutron Source (SINQ), the Spallation Neutron Source at Oak Ridge National Laboratory (SNS) and those of future Accelerator Driven System (ADS) devices, the target materials for producing neutrons are heavy liquid metals such as Hg, liquid Pb or liquid Pb–Bi eutectic (LBE). The advantages of utilizing liquid metals as targets are mainly: (1) damage produced by energetic protons and spallation neutrons in solid target materials such as W and Ta used in ISIS (the English Spallation Source) can be avoided; (2) radioactive waste from spent targets can be reduced as the liquid metals can be reused; and (3) the heat deposited in target materials can be easily removed. However, the use of liquid metals also introduces some disadvantages. A major one is liquid metal induced corrosion and embrittlement effects on structural (e.g. container, pipes etc.) materials, in particular under intensive irradiation.

The scientific support studies of MEGAPIE [1,2] demonstrate that at temperatures below 400 °C, the corrosion effects of LBE on ferritic/martensitic (FM) and austenitic steels are not so severe while the embrittlement of LBE on FM steels can occur, especially in a temperature range of 200–400 °C and for hardened materials. For the MEGAPIE target, the temperature at the beam window of the LBE container (made of the T91 steel) ranges from 250 to 340 °C. It is, therefore, considered that the corrosion effects may not be an important issue, while the embrittlement effect has to be investigated.

In the second irradiation experiment of the SINQ Target Irradiation Program (STIP-II), four capsules made of martensitic steel 9Cr2WVTa and austenitic steel EC316LN were irradiated to doses up to 18 dpa in contact with either Hg or LBE at temperatures up to about 350 °C [3]. In addition, the capsules were filled with aluminum to induce stress when they were heated by the proton beam. The objective was to study irradiation assisted stress corrosion cracking (IASCC) for FM and austenitic steels applied in liquid metal spallation targets. For developing the MEGAPIE target, the capsules irradiated in LBE were inspected. The results of the inspections are presented in this paper.

2. Experimental

2.1. Materials and specimens

The capsules were supplied by the Oak Ridge National Laboratory (ORNL), USA. They were fabricated from the 9Cr2WVTa and EC316LN steels which were taken as representatives of FM and austenitic steels, respectively. The compositions of the materials are given in Table 1.

Fig. 1 shows the drawings and picture of a capsule. The exact fitting Al-rod was shrink-fit in the capsule. The end-plug was sealed

* Corresponding author. Tel.: +41 56 310 4171; fax: +41 56 310 4529.
E-mail address: yong.dai@psi.ch (Y. Dai).

0022-3115/$ - see front matter © 2008 Elsevier B.V. All rights reserved.
doi:10.1016/j.jnucmat.2008.02.051

Table 1
Compositions (wt%) of the 9Cr2WVTa and EC316LN steels

Steel	Fe	Cr	Ni	Mo	Mn	C	Si	N	W	V	Ta
9Cr2WVTa	Bal	8.71	0.02	<0.01	0.39	0.098	0.19	0.016	2.17	0.23	0.06
EC316LN	Bal	17.45	12.2	2.5	1.81	0.024	0.39	0.067			

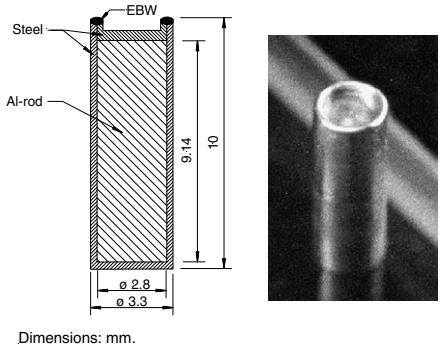

Fig. 1. Sketch and picture of the Al-stressed capsule.

with electron beam (EB) welding. Four such capsules, two of 9Cr2WVTa and two of EC316LN were irradiated in Rod-B of STIP-II together with some other specimens (tensile, B-fatigue, TEM disks). All the specimens were carefully packed in a few sample fixtures and then in a specially designed sample holder, and then submerged into liquid LBE at about 150 °C. After taking out the filled holder from the LBE bath and cooling down to room temperature, a rod with LBE, specimens and sample-fixtures (of the T91 steel) was cast. This rod was then inserted into a capsule (of T91) as shown Fig. 2. After sealing with laser welding, the whole capsule was inserted into a SS 316L tube and finally finished as normal target rods with EB weld sealing. The structure of this special rod (Rod-B) is illustrated by the sketch in Fig. 2. It should be noted that the T91 capsule was essentially a protection capsule. There was ~10% free volume inside this capsule, which would allow the expansion of LBE and accumulation of gases (He, H etc.), so that the capsule would not be over-stressed. Another point is that the LBE-filling was conducted at about 150 °C in order to ensure no serious oxidation of the specimens during the filling and relatively low oxygen content (~ the saturation level at 150 °C) in the LBE. The capsules investigated in this work are the two in Cell 3. The left one is an EC316LN capsule and the right one is a 9Cr2WVTa capsule.

2.2. Irradiation

The STIP-II irradiation was performed in SINQ Target-4 during 2000 and 2001 [3]. The proton charge received by the target was 10.03 Ah. The irradiation parameters such as proton and neutron fluences, displacement damage (dpa) and helium (He) and hydrogen (H) values were calculated with the MCNPX code using the profile of the accumulated proton fluence evaluated by gamma-mapping performed on the beam entrance area of the $AlMg_3$ container. To validate the calculated values, He and H contents were measured from a number of specimens at the Pacific Northwest National Laboratory (USA) [4,5]. The results indicated that the measured He values agreed roughly with the calculated ones. The measured H concentrations were, in most specimens, much lower than the calculated ones particularly for specimens irradiated at above 200 °C due to fast diffusion of H. The irradiation dose at the middle position of the EC316LN capsule was 16.7 dpa and at the 9Cr2WVTa capsule was 12.2 dpa, and the corresponding He concentrations were about 1695 and 1050 appm, respectively.

The irradiation temperature was monitored during irradiation with several thermocouples installed in different specimen rods.

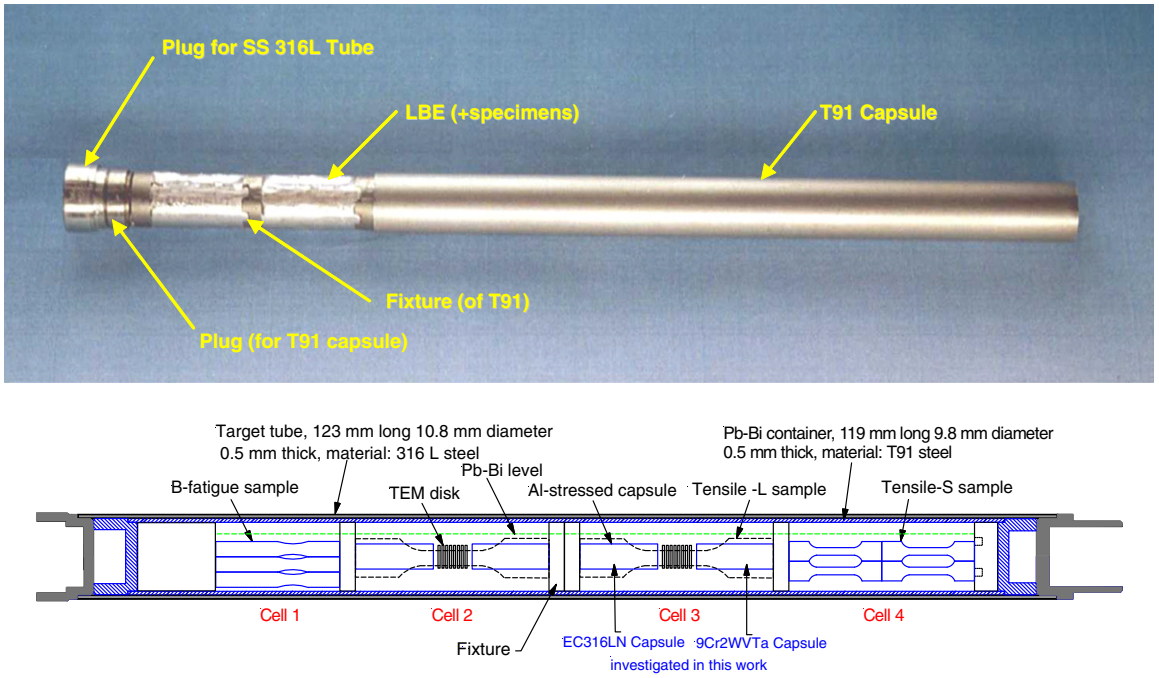

Fig. 2. Photo and sketch of the specimen loaded in Rod-B of STIP-II.

As the specimens were heated mostly by the energy (~90%) deposited by incident protons, the irradiation temperature varied along the longitudinal axis of a specimen rod as the proton beam intensity had a 2D-Gaussian distribution with sigma ≈2.6 cm for the major axis and sigma ≈2.1 cm for the minor axis. Meanwhile, the proton beam current was not constant during the two-year irradiation period and varied in a range from 0.9 mA to 1.25 mA (the mean value was about 1.1 mA), which resulted in a variation of ±15% around the mean irradiation temperature. The temperature of each individual specimen was calculated using the ANSYS code. Fig. 3 presents an example of the temperature distribution on the cross-section of the 9Cr2WVTa capsule calculated using a slightly simplified model and for an energy deposition (in steel) of 280 W/cm^3 case (equivalent to 1.1 mA proton beam current). The calculation indicated that the mean irradiation temperature of the EC316LN capsule varied from 335 °C at one end to 290 °C at the other end, and for the 9Cr2WVTa capsule it varied from 255 °C to 195 °C.

The stress distribution in the walls of the capsules was rather complicated due to the inhomogeneous temperature distribution inside the capsules. The difference of thermal expansion between the Al and the steels stressed the walls of steel capsules mainly in the longitudinal direction while the hoop stress was much smaller when the capsules were heated up [6]. Assuming the Al-rods fitted perfectly in the capsules, a simple calculation using the linear thermal expansion model showed that the deformation in the walls of the capsules induced by the Al-rods would be about 0.2% for the EC316LN capsule at 315 °C (the averaged temperature) and about 0.27% for the 9Cr2WVTa capsule at 225 °C. Considering the 0.2%-off-set yield strength being about 160 MPa for the EC316LN at 315 °C [7] and about 620 MPa for the 9Cr2WVTa steel at 225 °C [8], and the Young's modulus being about 175 GPa for SS 316 steels and about 200 GPa for FM steels at the corresponding temperatures, it is expected that the EC316LN capsule was plastically deformed and stressed at a level of about 160 MPa, while the 9Cr2WVTa capsule was stressed at about 540 MPa and very little plastic deformation is expected. The high stresses existing at the beginning of the irradiation were gradually relaxed by irradiation creep (thermal creep might be negligible at such low temperatures) afterwards. This will be further discussed in the next section.

More detailed information about the STIP-II irradiation can be found in [3].

2.3. Neutron radiography and visual inspections

After irradiation all the specimen rods were extracted from the target in a hot-cell nearby the SINQ target station. Most of the rods were first inspected with the neutron radiography technique available at SINQ. Afterwards all the rods were transferred to a hot-cell in the PSI hot laboratory, where the specimens were unpacked and sorted. The specimens in Rod-B were extracted by melting the LBE at about 150 °C. They were then visually inspected with a periscope installed in the hot-cell.

2.4. Electron probe microanalysis (EPMA)

Finally, the capsules were embedded horizontally with the sample fixtures in epoxy resin and ground down to its middle for analyzing their cross sections. The polishing was finished with 1 μm diamond suspension. A view of the prepared specimen is given in Fig. 4.

The specimen cross-section was analyzed with a fully shielded CAMECA-SXR-50 electron probe microanalysis (EPMA) device equipped with four spectrometers and operated at 20 keV. Secondary electron (SE) imaging and elemental semi-quantitative dot mapping were conducted on the specimens.

3. Results and discussion

3.1. Neutron radiography

The results of neutron radiography inspections before and after irradiation are presented in Fig. 5. It should be noted that due to the high activity of the rod, the imaging technique applied after irradiation did not deliver as good pictures as the one used before irradiation. The image looks more blurred. Nevertheless, the specimens, even the small TEM discs, 0.25 mm thick, can still be clearly recognized. The stressed capsules can also be seen. This indicates that these specimens might not be significantly corroded as compared to the ones irradiated in contact with Hg [3]. The position of the specimens changed slightly after irradiation, which suggests that the LBE was completely melted during irradiation.

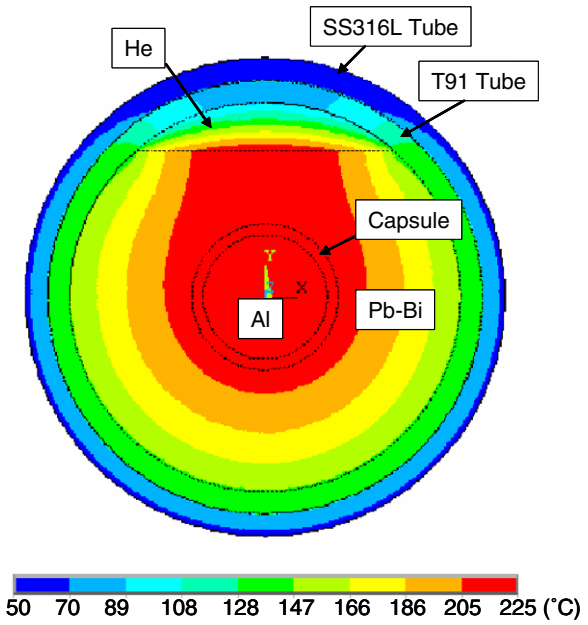

Fig. 3. Temperature distribution on the cross-section of a 9Cr2WVTa capsule calculated with the ANSYS code for the energy deposition (in steel) of 280 W/cm^3 case.

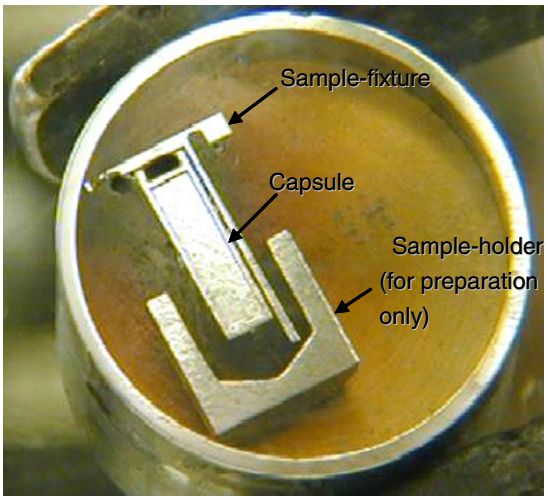

Fig. 4. A picture showing the polished cross-section of the 9Cr2WVTa steel capsule.

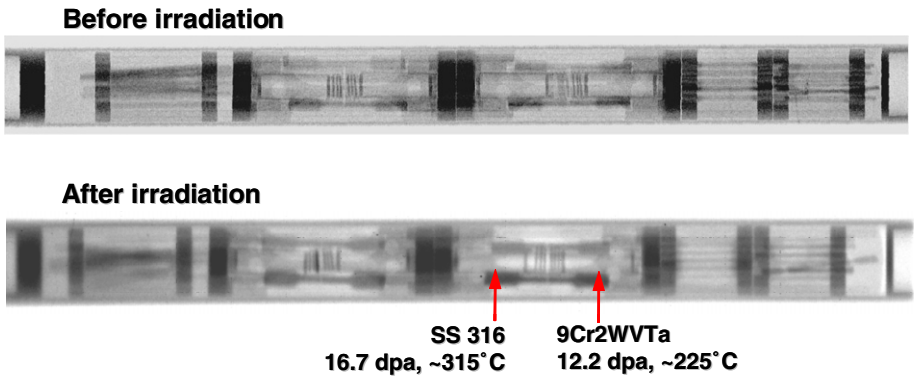

Fig. 5. Neutron radiography of Rod-B (STIP-II) before and after irradiation.

3.2. Visual inspections

After melting the LBE and pushing the sample package out of the T91 protection capsule, the samples were inspected with a periscope and some pictures were taken. Fig. 6(a) shows the sample package obtained from Cell 3 (Fig. 2). One can see that quite a lot of Pb–Bi remained on the surfaces of the specimens. However, some areas look Pb–Bi free. After removing the tensile samples, the capsules could be clearly seen. Similarly, their surfaces were mostly covered by Pb–Bi. As can be seen in Fig. 6(b), the visual inspections confirmed that no obvious damage occurred to the capsules.

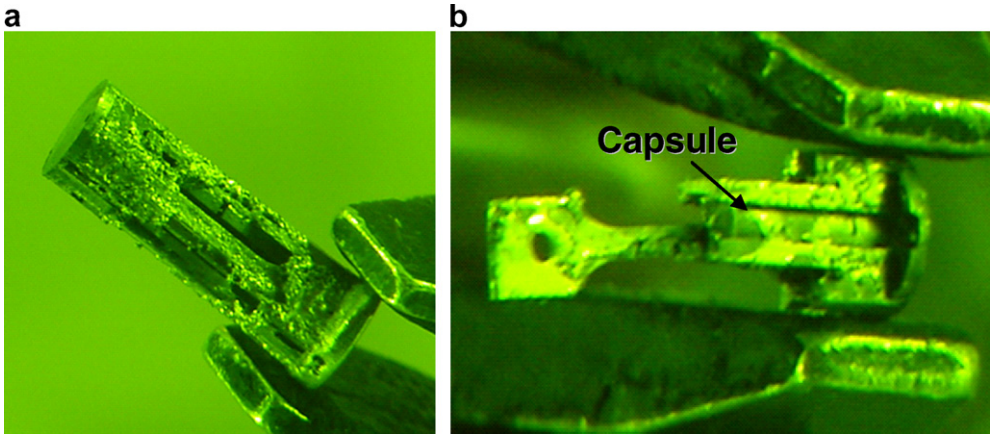

Fig. 6. Pictures of (a) the sample package in Cell 3 and (b) the 9Cr2WVTa capsule with a neighbor tensile specimen after irradiation.

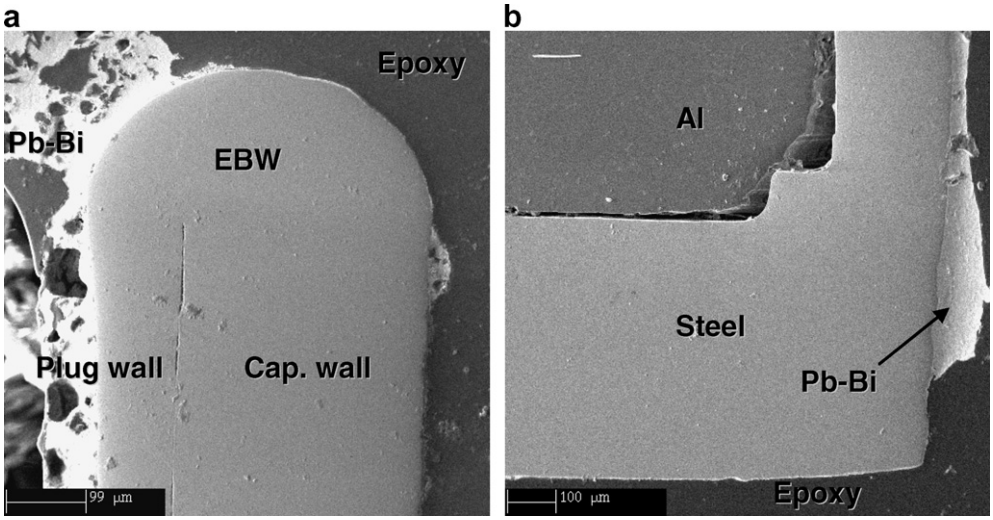

Fig. 7. Micrographs showing two positions in the EC316LN capsule: (a) the EBW at the top and (b) the corner at the bottom.

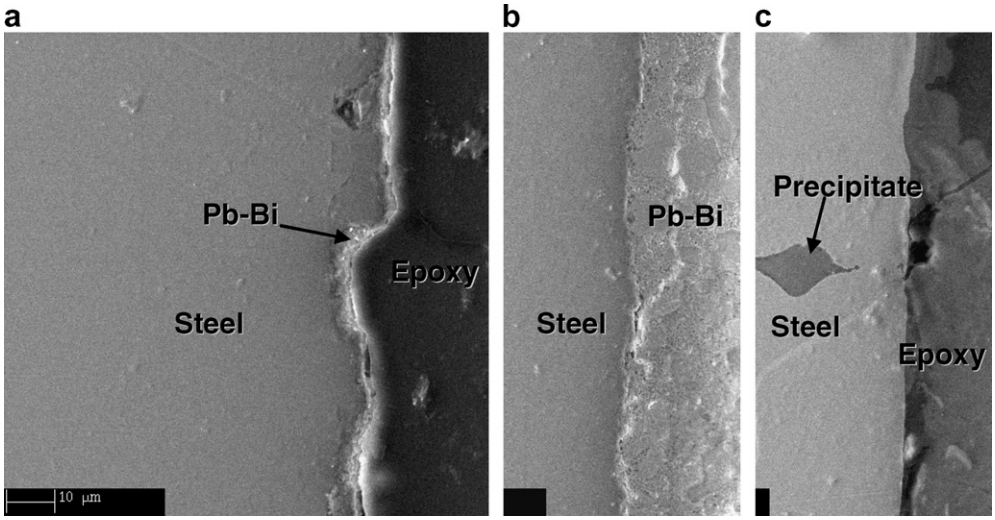

Fig. 8. Micrographs showing views of three areas of the EC316LN capsule: (a) the largest damage observed on the surface, (b) a view of an area with adherent Pb–Bi, and (c) a view of an area almost Pb–Bi free. The scale is the same for (a), (b) and (c).

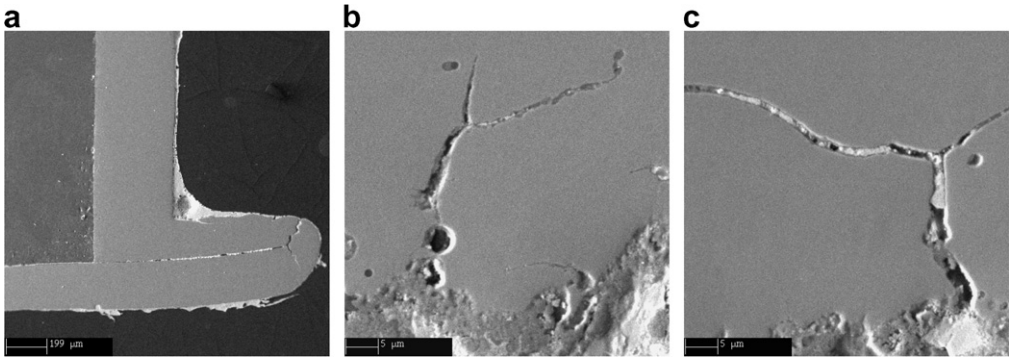

Fig. 9. Micrograph showing cracks observed in the 9Cr2WVTa capsule in different areas of (a) the EBW and (b) and (c) the vicinity of the EBW.

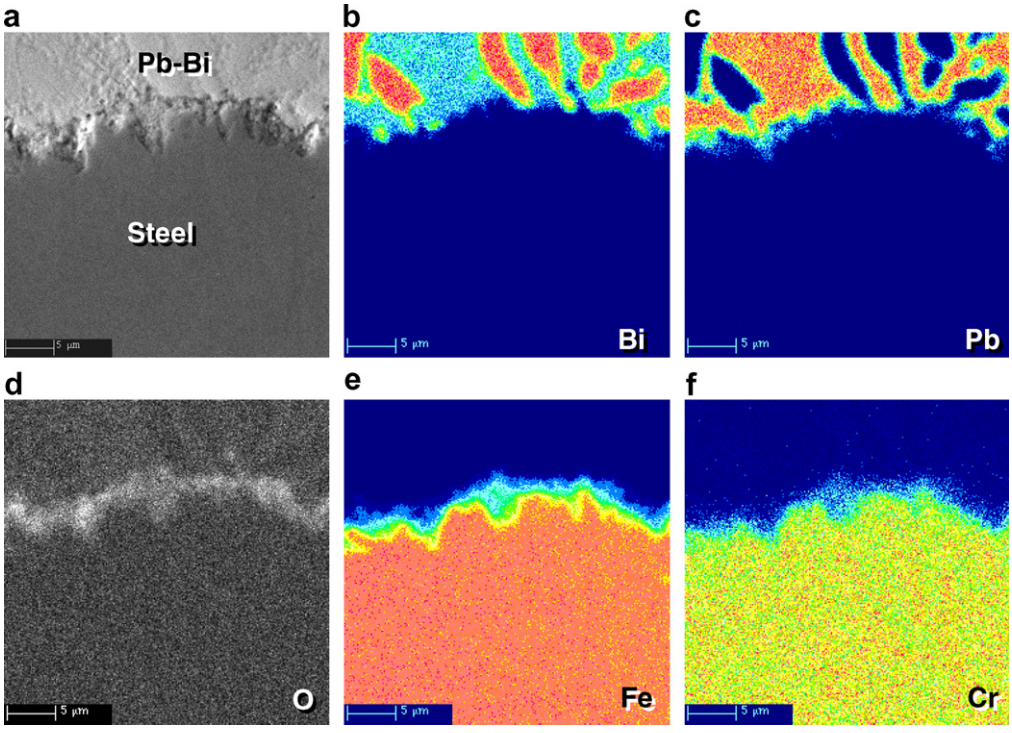

Fig. 10. Micrograph and element mapping of the surface of the 9Cr2WVTa capsule.

3.3. EPMA inspections

3.3.1. The EC316LN capsule

An overview of the capsule indicated that there was a large gap of about 50 μm in width located at the top between the Al-rod and the steel wall, and a small gap of 5–10 μm at the bottom but almost no gap at the side. This suggests that the capsule underwent a quite large deformation resulting probably from both the plastic deformation and irradiation creep.

One of main features is that no cracks were observed in the wall of the capsule. Fig. 7 illustrates two positions of the capsule, the EBW at the top and the corner at the bottom, where higher stresses existed. Although the stress was quite large at the beginning of the irradiation, it should be quickly relaxed by irradiation creep. Taking an irradiation creep rate of 1.3×10^{-4} MPa^{-1} dpa^{-1} obtained from SS 316 irradiated with neutrons at 330 °C [9], the stress could be reduced to less than 10 MPa at a dose below 1 dpa, which means within one month after starting irradiation. In addition, the EC316LN steel has good radiation damage resistance [7]. Therefore, it is understandable that no cracks were observed.

Observations at high magnifications revealed another important feature: no severe corrosion damage. Fig. 8 shows the views from three different areas: (a) the most evident damage observed on the surface, (b) a view of areas with adherent LBE, and (c) a view of areas almost LBE free. The large roughness in (a) is suspected to be produced by fabrication, while the view shown in (b) is considered as a representative of the surface slightly corroded by LBE. The view in (c) indicates that some areas were not wetted by the LBE. Elemental analysis suggests that no or a very thin (<1 μm) oxide layer was on the surface. Anyhow, the largest corrosion depth is about 10 μm, if the rough surface shown in (a) was produced by corrosion. This is relatively small compared with the corrosion damage observed from SS 316 L exposed to flowing LBE at 400 °C [10] or stagnant LBE at 550 °C [11] for shorter durations of about 2000 h. Furthermore, unlike the cases in [10,11] no grain-boundary penetration occurred. The reasons are most probably the lower temperature and a stagnant LBE environment. Another possible reason is that the oxygen content in the capsules might be higher than that in [10] 10^{-8}–10^{-10} wt%, or in [11] 3.9×10^{-9} wt%.

3.3.2. The 9Cr2WVTa capsule

The situation of the 9Cr2WVTa capsule is quite different from that of the EC316LN capsule. The first evidence is the observation of cracks in the EBW and its vicinity of the capsule, as shown in Fig. 9. Unfortunately, no similar capsules were available for checking cracks before irradiation. But cracks in an EBW of a FM steel are seldom observed. Therefore, it is believed that the cracks could be essentially attributed to two reasons: the high stress level and the brittle material.

As mentioned in the previous section, the stress in this capsule was about 540 MPa at the beginning of the irradiation. Since the temperature was low, the thermal creep could be negligible. Due

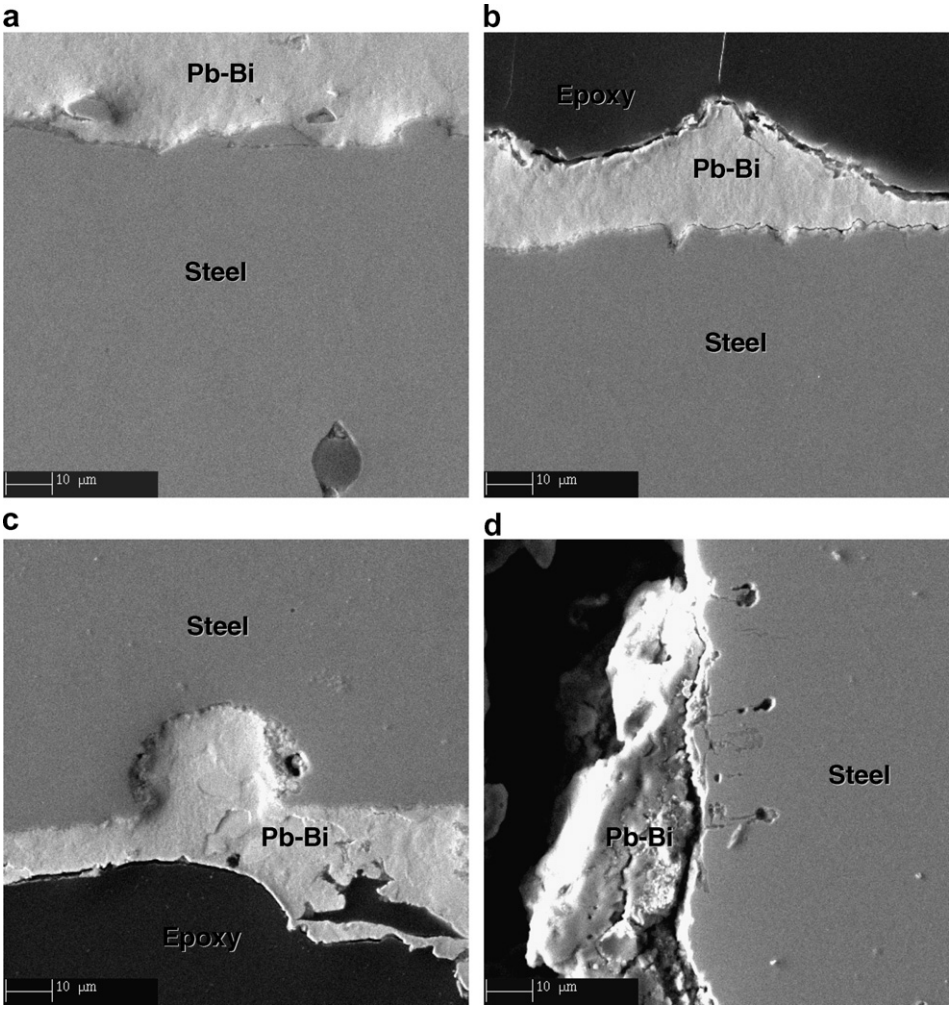

Fig. 11. Micrographs showing some interesting morphology features on the 9Cr2WVTa capsule.

to the lack of irradiation creep data from spallation irradiation, we can only use neutron irradiation data to evaluate the irradiation creep induced stress relaxation. Recently, irradiation experiments on some FM steels performed at 300 °C in the high flux isotope reactor in USA (HFIR) demonstrated that the irradiation creep rate of FM steels increased linearly with stress up to about 275 MPa, and rose very quickly with increasing stress at above 320 MPa [12]. The irradiation creep rate at <300 MPa was about 0.7×10^{-6} MPa^{-1} dpa^{-1}. Assuming the stress of the 9Cr2WVTa capsule could be quickly reduced to 300 MPa, a further reduction from 300 MPa to 100 MPa would require an irradiation dose of about 3 dpa, which means nearly 3 months of irradiation time for this capsule. In this case, it is believed that the capsule remained at a relatively high stress level for a relatively long period of time after starting irradiation.

On the other hand, it is expected that re-tempering after welding was not performed to this capsule in order to avoid any deformation before irradiation induced by thermal stress. Hence, like non-tempered FM steels, in the EBW region the material was very hard and brittle. The large crack in the EBW (Fig. 9(a)) propagated from inside and should be resulted from a combined effect of the brittleness of the EBW material and the high stress or, more precisely, the high stress concentration at the tip of the gap between the walls of the plug and the capsule tube. While the micro-cracks shown in Fig. 9(b) and (c) propagated from the outer surface, which could be due to the embrittlement effect of LBE. Our recent studies on liquid metal embrittlement effects of LBE on the T91 steel demonstrated that hardened specimens presented much higher susceptibility of embrittlement when high stress and surface flaws existed in the specimens [13,14]. The material in the region where the micro-cracks were observed could be hardened by either welding (in or very close to the heat-affected zone) or irradiation. Micro-cracks could be readily initiated at sites of precipitates on the surface or fabrication flaws, and their propagation would be driven by the embrittlement effect of LBE.

The observations give also clear evidence of corrosion even though the irradiation temperature was low. The roughness of the surface observed on the 9Cr2WVTa capsule (Fig. 10(a)) indicates slightly higher corrosion rate than in the EC316LN capsule (Fig. 8(b)). Fig. 10(b)–(f) shows the element (Bi, Pb, O, Fe and Cr) mapping results. Fig. 10(d)–(f) indicates an oxide layer formed on the surface, as it is usually observed in LBE corrosion tests of FM steels [15–17] at a medium or high oxygen content level.

There were some other interesting observations, as shown in Fig. 11. The micrographs in Fig. 11(a) and (b) present features that are considered as a combined effect of corrosion and fabrication. The rough surface was most likely produced by fabrication. During irradiation some small pieces (e.g. the small island in Pb–Bi at the upper-left corner of Fig. 11(a)) were spalled from the surface by corrosion. Fig. 11(c) and (d) and also Fig. 9(b) demonstrate that precipitates at the surface or in the surface layer may enhance corrosion penetration into the steel matrix.

Last, not least, the observation showed that the surface was mostly covered by Pb–Bi, which indicates the wetting of LBE to the 9Cr2WVTa steel at such low temperatures (195–255 °C) under irradiation.

4. Conclusions

Stressed capsules of EC316LN and 9Cr2WVTa steels were irradiated in contact with static LBE to 16.7 and 12.2 dpa at 315 and 225 °C, respectively, for studying LBE corrosion effects under intensive proton and neutron irradiation. The capsules were investigated using the EPMA technique. The results demonstrate that:

(1) No cracks were observed from the EC316LN capsule. It is believed that the stress in the capsule wall was relaxed quickly after starting irradiation, within one month at <1 dpa.
(2) Cracks were observed in the EBW and its vicinity in the 9Cr2WVTa capsule. The cracks in the EBW started from the tip of the gap between the walls of the plug and the capsule tube, which can be attributed to the high stress and the brittle nature of the weld. The cracks on the outer surface may associate with LBE induced embrittlement effects.
(3) Corrosion depth was less than 10 μm in general for both capsules. The 9Cr2WVTa steel capsule showed slightly more severe corrosion than the EC316LN steel capsule even at lower temperature and dose.
(4) Precipitates at the surface of the 9Cr2WVTa steel capsule induced large pits under corrosion and irradiation, and further initiated cracks under stress.

Acknowledgements

Dr E.H. Lee (ORNL) is acknowledged for supplying the samples. Mr K. Geissmann, Mr R. Thermer and Ms A. Waelchli (PSI) are acknowledged for their help on irradiation and sample preparation work. Drs H. Hou (North University of China), H. Wang (China Institute of Atomic Energy) and A. Alam (PSI) are acknowledged for their help on temperature and stress calculations.

References

[1] Y. Dai, J. Henry, T. Auger, J.B. Vogt, A. Almazouzi, H. Glasbrenner, F. Groeschel, J. Nucl. Mater. 356 (2006) 308.
[2] J. Henry et al., Structural materials for the MEGAPIE target, CEA technical report: DMN/SRMA/LA2M/NT/2006-2761/A.
[3] Y. Dai, X. Jia, R. Thermer, D. Hamaguchi, K. Geissmann, E. Lehmann, H.P. Linder, M. James, F. Gröschel, W. Wagner, G.S. Bauer, J. Nucl. Mater. 343 (2005) 33.
[4] Y. Dai, Y. Foucher, M.R. James, B.M. Oliver, J. Nucl. Mater. 318 (2003) 167.
[5] B. Oliver, Y. Dai, R.A. Causey, J. Nucl. Mater. 256 (2006) 148.
[6] M. Ashrafi-Nik, Thermo-mechanical analysis of the STIP-V sample, PSI technical report: TM-34-06-03, 2006.
[7] Y. Dai, J. Egeland, B. Long, J. Nucl. Mater. 377 (2008) 109.
[8] R.L. Klueh, Experience with ferritic/martensitic steels for fusion application, in: Proceedings of the International Workshop on Spallation Materials Technology, Oak Ridge, USA, 1996, p. 3.3.
[9] M.L. Grossbeck, L.K. Mansur, M.P. Tanaka, in: N.H. Packen, et al., (Ed.), Effects of Radiation on Materials, 14th International Symposium on ASTM STP 1046, Philadelphia, 1990, p. 537.
[10] A. Aiello, M. Azzati, G. Benamati, A. Gessi, B. Long, G. Scaddozzo, J. Nucl. Mater. 335 (2004) 169.
[11] F. Gnecco, E. Ricci, C. Bottino, A. Passerone, J. Nucl. Mater. 335 (2004) 185.
[12] M. Ando, M. Li, H. Tanigawa, M.L. Grossbeck, S. Kim, T. Sawai, K. Shiba, Y. Kohno, A. Kohyama, J. Nucl. Mater. 367–370 (2007) 122.
[13] B. Long, Y. Dai, F. Groeschel, J. Nucl. Mater. 377 (2008) 219.
[14] B. Long, Y. Dai, F. Groeschel, J. Nucl. Mater. 376 (2008) 341.
[15] F. Barbier, A. Rusanov, J. Nucl. Mater. 296 (2001) 231.
[16] C. Fazio, G. Benamati, C. Martini, G. Palombarini, J. Nucl. Mater. 296 (2001) 243.
[17] Y. Dai, H. Glasbrenner, V. Boutellier, R. Bruetsch, X. Jia, F. Groeschel, J. Nucl. Mater. 335 (2004) 232.